Low-temperature properties and ESR in the quasi-one-dimensional random compound $MnMgB_2O_5$

J. C. Fernandes, R. B. Guimarães, and M. A. Continentino*
Instituto de Física, Universidade Federal Fluminense, Campus da Praia Vermelha, 24210-340 Niterói, Rio de Janeiro, Brazil

R. Rapp
Instituto de Física, Universidade Federal do Rio de Janeiro, Caixa Postal 68528, 21945-970 Rio de Janeiro, Rio de Janeiro, Brazil

J-L. Tholence and J. Dumas
Laboratoire d'Etudes des Propriétés Electroniques des Solides, CNRS, Boîte Postale 166, 38042 Grenoble, Cedex 9, France

Y. Blancquaert, S. Yates, and C. Paulsen
Centre de Recherches sur les Très Basses Températures, CNRS, Boîte Postale 166, 38042 Grenoble, Cedex 9, France
(Received 11 July 2003; revised manuscript received 17 October 2003; published 20 February 2004)

Low-temperature magnetization, ac susceptibility, and specific heat have been measured on powdered $MnMgB_2O_5$ between 100 mK and 6.8 K. A power-law temperature dependence of the susceptibility has been found down to 2 K in agreement with previous measurements. The exponent describing this behavior is close to that found for the warwickite $ScMnOBO_3$, another Mn^{2+} compound with a similar low dimensional random magnetic arrangement of Mn ions. The magnetic and specific-heat measurements indicate that, below 600 mK, the $MnMgB_2O_5$ pyroborate freezes in a glassy state. Electron-spin resonance measurements (ESR) on a single crystal of this compound are also presented. The linewidth and the *g* factor show different temperature dependencies for different directions of the applied field. Finally a theory is presented for ESR in random exchange Heisenberg antiferromagnetic chain (REHAC) compounds.

DOI: 10.1103/PhysRevB.69.054418 PACS number(s): 75.20.Ck, 75.60.Ej, 76.30.−v

I. INTRODUCTION

This work presents an investigation of the low-temperature magnetic and thermodynamic properties of the pyroborate $MnMgB_2O_5$ compound. Magnetization, ac susceptibility, specific heat as well as the electron-spin resonance (ESR) parameters are presented as a function of temperature. A theory for explaining the temperature dependence of the ESR linewidth and *g* factor in the framework of a random chain compound is also given.

The crystalline structure of $MnMgB_2O_5$ has been studied by Utzolino and Bluhm.[1] It is triclinic with space group *P*-1 (number 2). The metal ions Mn^{2+} and Mg^{2+} are found inside oxygen octahedra that share edges and form substructures such as *ribbons*, four rows wide, as shown in Fig. 1. These ribbons are parallel to the crystal *a axis* and contain two distinct crystallographic sites for the metal ions. Both ions occupy the two metal sites so that this compound is *intrinsically* disordered. Metal spins in neighbor ribbons interact through the *super-super-exchange* mechanism while the spin interaction between neighbor ions within the same ribbon is mainly due to the *super-exchange* mechanism, as this is an electrically insulating material.

In a recent paper Fernandes *et al.*[2] have measured the ac susceptibility and the magnetization of the *heterometallic* pyroborate $MnMgB_2O_5$, down to 2 K. This study also presented measurements for the *homometallic* isomorph pyroborate $Mn_2B_2O_5$. The latter shows antiferromagnetic order below 23.3 K while the heterometallic pyroborate has a behavior typical of random exchange Heisenberg antiferromagnetic chain (REHAC) systems below 19 K. This is characterized by a power-law dependence of the susceptibility on temperature and of the magnetization on the applied field for high fields. No magnetic order was found in the former system down to the lowest temperatures (2K) attained in this study.

In this work we present magnetization, ac susceptibility, and specific-heat measurements, down to approximately 100 mK, as a tentative to observe magnetic ordering of the heterometallic pyroborate. We have observed that this magnetic system actually freezes below 600 mK in a magnetic glass state which is destroyed by field cooling under 100 Oe. The

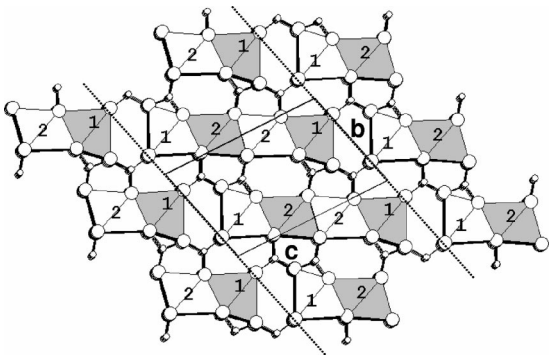

FIG. 1. The structure of the pyroborates projected in the plane *bc*, from Ref. 2. We may notice the ribbons, the borate groups, and the sides *b* and *c* of the unit cell. The largest circles indicate oxygen ions while the smallest ones indicate boron ions. The dashed lines indicate one column of ribbons. The *a* coordinates of metal 1 and metal 2 sites within dark octahedra are the same while the clear ones differ from those by *a*/2.

magnetization curve at 100 mK shows a small hysteresis due to a small magnetic component freezing in the direction of the magnetic field. Another goal of the present study is to compare the main features of ESR measurements in this inorganic insulating REHAC, with those obtained by Tippie and Clark[3] on quinolinium $(TCNQ)_2$, a well studied organic REHAC conductor. The overall behavior of ESR is very similar in both systems in spite of the different magnitudes of linewidths in each compound. In the pyroborate the linewidths are more than two orders of magnitude greater than those in quinolinium $(TCNQ)_2$. To the best of our knowledge this paper presents the first ESR measurements in an inorganic REHAC. These systems are the subject of intensive investigations mostly from the theoretical point of view.[4] The thermodynamic properties and ground state of spin-1/2 REHAC are now well known. However the expected physical behavior of REHAC systems with $S>1/2$ is still under intense debate.[4] For this reason it is very important to have as many as possible candidate systems and results for these kind of material. The heterometallic pyroborate investigated here provides unambiguous experimental evidence for the existence of a Griffiths phase in this $S=5/2$ REHAC material. The Griffiths phase consists of singlet pairs with a large distribution of exchange couplings which form along the ribbons.

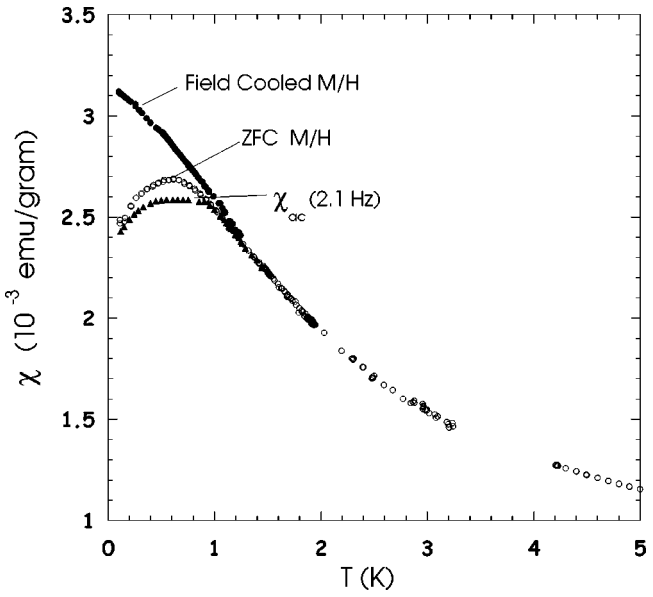

FIG. 2. The (M/H) vs temperature curves, at 100 G, for field-cooled (FC) and warm-up zero-field-cooled (ZFC) regimes. Also shown is the real part of the ac susceptibility vs temperature curve for $MnMgB_2O_5$ at 2.1 Hz. Similar curves are obtained for 0.21 and 21 Hz.

II. EXPERIMENT

A. The sample

The sample has been synthesized following the method presented in Ref. 2. For the ESR measurements we have employed an as grown single crystal whose size is circa $0.5\times0.8\times2$ mm^3. The crystalline structure has been identified through x-ray powder diffraction. We used a powdered sample for susceptibility and specific-heat measurements.

B. Susceptibility and Magnetization

The low-temperature magnetization and ac susceptibility measurements were made using a low-temperature high-field SQUID magnetometer developed at the CRTBT in Grenoble. A miniature dilution refrigerator was used to reach temperatures down to 90 mK. A powder sample of $MnMgB_2O_5$, weighting 19.5 mg, was mixed with a small amount of apiezon grease and squeezed into a small copper pouch. The sample and pouch were thermally anchored to a copper coil foil sample holder suspended from the bottom of the mixing chamber of the dilution refrigerator. During measurements, the sample was extracted through the gradiometer coils of a superconducting flux transformer coupled to the SQUID. In this way absolute value measurements were made.

Figure 2 shows the M/H dc susceptibility between 100 mK and 5 K in field-cooled (FC) and zero-field-cooled (ZFC) regimes, respectively, both under an applied field of 100 G. The ac susceptibility, χ_{ac}, vs temperature curve, for 2.1 Hz, also appears in this figure. There is a very broad peak in the ac susceptibilities and in the warm-up ZFC magnetization curves. For the ac data the peak position has a very weak frequency dependence consistent with a spin glass-like ordering below 600 mK. Moreover specific-heat measurements down to very low temperatures to be presented below, show no anomaly in this temperature region clearly ruling out long-range magnetic ordering. The imaginary parts of the ac susceptibility for different frequencies is very small. Figure 3 shows the M vs H curves for 100 mK and 4.2 K with H running between 0 and 1000 G. At 100 mK there is a slight hysteresis possibly due to a small magnetic component freezing in the direction of the applied field. The linearity at these low fields is not surprising. Figure 4, the last of this subsection, shows the $\ln(M/H)$ vs $\ln(T)$ curve under 100 G for ZFC. From this curve we conclude that, down to 2 K, $\chi_{dc} \propto T^{-\alpha}$ where $\alpha=0.56$. This result agrees with the previous

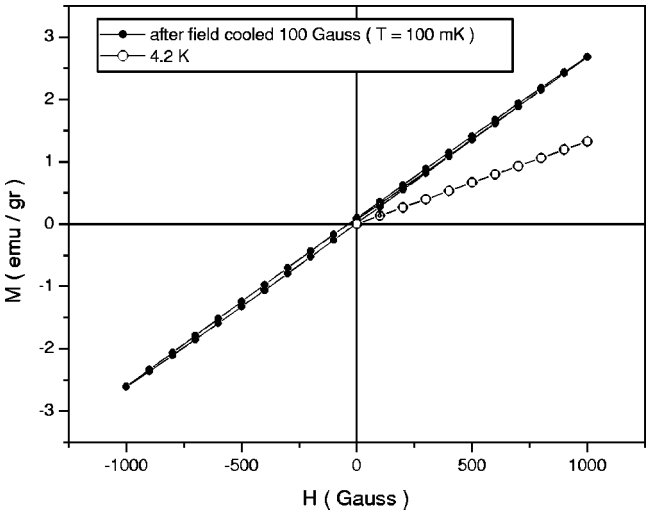

FIG. 3. Field dependence of magnetization for $MnMgB_2O_5$ at 100 mK and 4.2 K. A slight hysteresis at 100 mK may be observed.

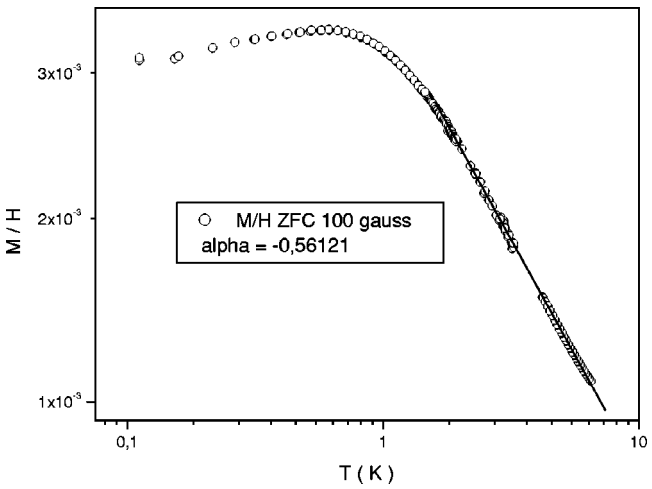

FIG. 4. Double logarithmic plot of (M/H) vs T curve for $MnMgB_2O_5$ from 100 mK to 6.8 K. A $\chi_{dc} \propto T^{-\alpha}$ law above 1 K is found with $\alpha = 0.56$ (full line).

measurements on this compound[2] which yield to $\alpha = 0.55$. This strongly suggests the existence of a Griffiths phase in this low dimensional random magnetic oxide above 1 K. Below this temperature a crossover to three dimensions occurs leading to the appearance of magnetic long-range order. It is important here to remark that the warwickite $MnScOBO_3$, a random chain compound with Mn^{2+} ions, also presents such a phase with an exponent $\alpha = 0.50$ in the low-temperature susceptibility.[6]

C. Specific heat

Specific heat measurements were performed using one calorimeter mounted in a dilution refrigeration cryostat (model DRI 420, SHE Corporation, USA) and covers the temperature range 0.08–3 K. Measurements were made using a semiadiabatic pulse method. The specific heat is measured with a relative uncertainty of 2%. The samples were prepared[7] as to improve the expected low thermal conductivity of the material. Powdered material, with particle size of about 100 μm, was mixed with a similar quantity of powdered copper with particle size of about 5 μm. The sample copper mixture wrapped with 0.04 mm thick copper foil, forming a chip, was compressed with about 25 MPa for about 30 min. The mass of the sample, copper, and grease were about 0.1, 0.2, and 0.002 g, respectively. In this way we obtained a good thermal conducting copper path around each sample particle, while keeping small the specific-heat background due to the added material. This provided a sample temperature equilibration time constant shorter than 60 sec in the full measuring range. This chip was glued with apiezon *N* grease to the calorimeter base copper plate, where the thermometer and heater were attached. When taking data, heat was applied to the sample during intervals of about 80 sec as to produce temperature changes of 5% of the sample temperature. The evolution of the temperature to equilibrium of the sample was measured during more than 500 sec. The specific-heat background of the calorimeter was determined in a separate measurement. The total heat capacity of the sample, C_{tot}, was obtained after subtracting to the measured value, the heat capacity of the calorimeter, the contributions of the copper powder and foil and the apiezon grease. The results are shown in Fig. 5. The heat capacity is a smooth function of temperature at the temperature where the susceptibility shows a maximum ruling out an antiferromagnetic transition. At very low temperatures the heat capacity rises with decreasing temperature due to a Schottky-like nuclear contribution associated with the 100% abundant isotope Mn^{55}.[8]

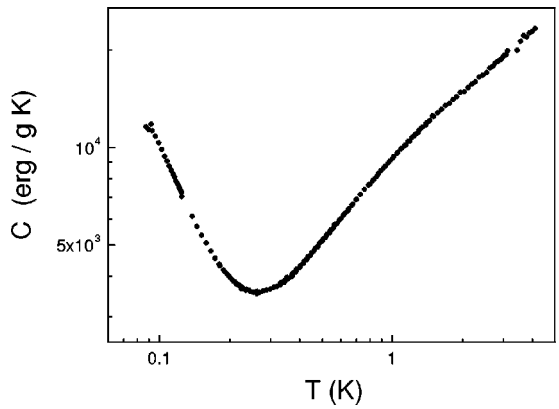

FIG. 5. Specific heat of $MnMgB_2O_5$ as a function of temperature.

D. ESR

ESR measurements were performed on a platelet of $MnMgB_2O_5$ whose dimensions are given above. A cw 9.5 GHz Brucker spectrometer was employed. The spectra have been taken, as a function of temperature, for dc applied field perpendicular and parallel to the largest edge of the platelet. Figure 6 shows the linewidth vs temperature curves for each orientation and the inset shows the low-temperature power-

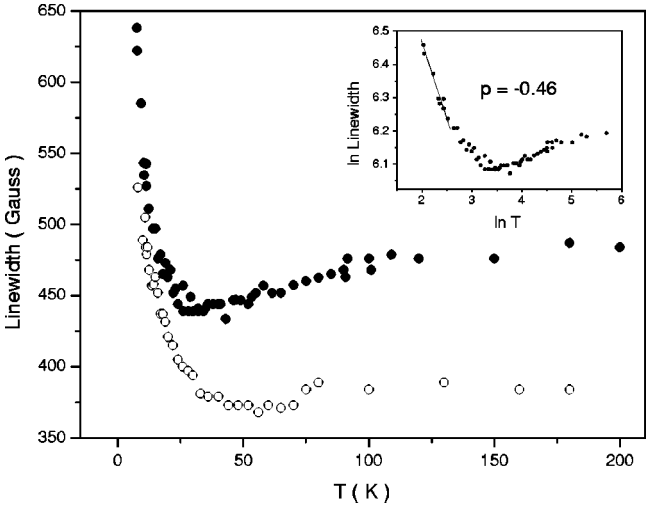

FIG. 6. Linewidth as a function of temperature for applied field parallel (filled circles) and perpendicular (open circles) to the direction of the ribbons. The inset shows the power-law behavior of the linewidth for the parallel direction.

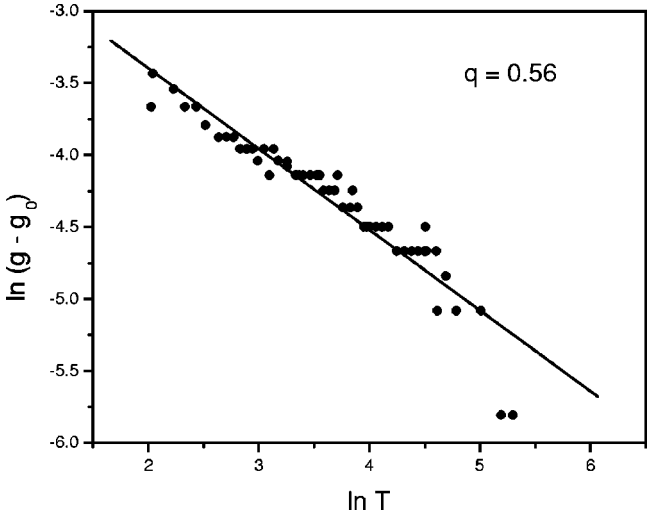

FIG. 7. The logarithmic plot of the g shift as a function of temperature for the applied field parallel to the ribbons' direction. The reference g factor $g_0=2.0161$ is that measured at room temperature. The linear fitting of the data yields an inclination $q=0.56$ close to the temperature exponent of the susceptibility.

law behavior. Linewidths have also been measured as a function of the angle between the applied field and the largest edge for both directions in the plane perpendicular to the largest face. At any field orientation and temperature the spectrum consists of a single intense, broad, and essentially symmetric Lorentzian line. We remark that the linewidths are larger for the applied field parallel to the largest edge of the platelet. This is the hard magnetization direction for $Mn_2B_2O_5$ as shown in Ref. 2. For the applied magnetic field parallel to this direction, the linewidth curve presents a minimum at 30 K (see Fig. 6) while, for applied field parallel to the two other edges of the platelet, the minima are found near 50 K. It is important to remark that the onset of the power law for the magnetic susceptibility is 19 K (Ref. 2), a temperature out of the range of the minima of the linewidth curves. These results must be compared with those obtained for quinolinium $(TCNQ)_2$, the above mentioned REHAC conductor. This compound orders magnetically at circa 1.5 mK (Ref. 5) and has ESR linewidths running between 0.05 G and 0.3 G below 20 K (Ref. 3). Although these quantities are very different from the corresponding ones in $MnMgB_2O_5$, the onset of the $T^{-\alpha}$ law for the susceptibility and the minimum of the linewidth vs temperature curve are very near to those for $MnMgB_2O_5$. They are 20 K (Ref. 9) and 25 K (Ref. 3), respectively. In both compounds the linewidths are larger for applied fields parallel to the chains' direction. In Fig. 7 we plot $\ln(g-g_0)$ vs $\ln T$ where $g_0=2.0161$ is the room temperature g factor. Notice that $g-g_0$ has a power-law behavior with temperature at low temperatures with an exponent very close to that found for the magnetic susceptibility.

III. THEORY FOR ESR IN RANDOM QUANTUM CHAINS

For an understanding of the temperature dependence of the ESR linewidth and g shift in this compound, we consider that the radio frequency (RF) is absorbed by $S=5/2$ *free* manganese ions in the chains. These ions, in an S state with zero angular momentum, absorb energy essentially at their Zeeman frequency in the applied external magnetic field. The relaxation of the energy absorbed from the RF source occurs via the weak coupling of the resonant ions to the singlet pairs forming a random singlet or Griffiths phase and from these to the lattice. The former interactions are dipolar or other kind of anisotropic coupling. We also assume that the random singlet pairs have a first excited state which couples to the lattice, such that, ultimately energy is transferred to this reservoir. This mechanism gives rise to a linewidth which can be written as[10]

$$\Delta H=\frac{D^2N}{g\mu_BN_0}\frac{1}{4kT}\mathrm{sech}^2(E/2kT)\frac{\omega\tau}{1+\omega^2\tau^2}, \tag{1}$$

where D is the anisotropic coupling of the free ions to the singlet pairs and ω is the resonance frequency. (N/N_0) is the *concentration* of pairs. The relaxation time τ of the pairs to the lattice quite generally depends on the energy E of the first excited state of the pair which is treated here as a two level system. These energies are random with a normalized probability distribution $P(E)$ which is essentially the distribution of the random exchange couplings of the singlet pairs given by[11]

$$P(E)=\frac{1}{Z\Omega}\left(\frac{E}{\Omega}\right)^{-\alpha},$$

where $\alpha=1-1/Z$ with Z the dynamic exponent[11] and Ω is the cutoff of the distribution. The average linewidth is given by,

$$\overline{\Delta H}=\frac{D^2}{g\mu_BZ\Omega}\int_0^\Omega\frac{dE}{4kT}\left(\frac{E}{\Omega}\right)^{-\alpha}\mathrm{sech}^2(E/2kT)\frac{\omega\tau(E)}{1+\omega^2\tau^2(E)}. \tag{2}$$

The E dependence of τ is determined by the particular mechanism of relaxation of the pairs to the lattice, the relevant dimension of the elastic array, etc. Here we shall neglect this explicit dependence and assume for simplicity an average relaxation time with a power-law dependence on temperature, i.e., $\overline{\tau}(T)=\tau_0(kT/\Omega)^{-z}$. The average linewidth can be written as,

$$\overline{\Delta H}=\frac{D^2}{g\mu_BZ\Omega}\left(\frac{kT}{\Omega}\right)^{-\alpha}\frac{\omega\overline{\tau}}{1+\omega^2\overline{\tau^2}}\int_0^{\Omega/kT}dy\,y^{-\alpha}\mathrm{sech}^2(y) \tag{3}$$

or, considering that the relevant low-temperature limit for this insulating material is $\omega\overline{\tau}\gg1$,

$$\overline{\Delta H}=\frac{D^2A(\alpha,\Omega/kT)}{g\mu_BZ\Omega(\omega\tau_0)}\left(\frac{kT}{\Omega}\right)^{-\alpha+z}, \tag{4}$$

where $A(\alpha,\Omega/kT)$ stands for the integral. The exponent α is obtained from the susceptibility measurements and for the present system is given by $\alpha=0.56$. Since the linewidth, as

shown in Fig. 5, behaves as $\overline{\Delta H} \propto T^{-p}$, with $p=-0{,}46$, we have from $p=\alpha-z$, that $z\approx 0.1$. This implies a very weak temperature dependence of the relaxation time of the singlet pairs to the lattice which however increases with decreasing temperature. Notice that this relaxation mechanism probably involve low dimensional phonons propagating along the ribbons.

The same mechanism responsible for the linewidth calculated above gives rise to a contribution to the g shift which is given by,[10]

$$\overline{\Delta g} = \frac{D^2 A(\alpha, \Omega/kT)}{\mu_B H_0 Z \Omega} \frac{\omega^2 \overline{\tau^2}}{1+\omega^2 \overline{\tau^2}} \left(\frac{kT}{\Omega}\right)^{-\alpha}, \qquad (5)$$

where H_0 is the room-temperature resonance field. In the low-temperature limit where $\omega^2 \overline{\tau^2} \gg 1$, the equation above yields a g shift which is frequency independent and has the same temperature dependence of the uniform magnetic susceptibility determined by the exponent $\alpha=-0.56$. This is indeed the case found experimentally, as shown in Fig. 6, lending further support to the proposed relaxation mechanism.

IV. DISCUSSION

In this paper we have presented magnetization, specific heat, and ESR results for the pyroborate system $MnMgB_2O_5$. This is an intrinsically disordered one-dimensional magnetic material. The low dimensionality is a consequence of the existence of ribbons in its structure which interact very weakly. Although the Mn^{2+} ions have a large magnetic moment, due to the random occupation of the metal sites in the low dimensional ribbons the system can only freeze and even so below 600 mK. This freezing is evident from a broad maximum in the susceptibility and the absence of a peak in the specific heat curve in the temperature range of this maximum. The magnetic behavior of this system above 2 K is characteristic of random exchange Heisenberg antiferromagnetic chains with a power-law behavior of the uniform susceptibility as a function of temperature and of the magnetization as function of the applied magnetic field. Such behavior is well documented in spin-1/2 REHAC systems where it is associated with the existence of a random singlet phase. However in spin-5/2 systems, as the case investigated here, it is not clear if such a phase does exist for strong disorder. Our results are consistent however with the existence of a Griffiths phase in this Mn pyroborate which gives rise to the power-law behavior with temperature independent exponents. In order to explain our ESR experiments, we have proposed a theory for the linewidth and g shift in this REHAC material. In this theory the energy absorbed of the radio-frequency field from free Mn ions is transferred to the lattice through the spin singlets associated with the Griffiths phase.

ACKNOWLEDGMENTS

This work has been supported by the Brazilian agencies FAPERJ, CNPq, and CNRS (France). Dr. C.O. Paiva-Santos has taken the x-ray diffractogram from $MnMgB_2O_5$ at the LIEC-UNESP.

*Electronic address: mucio@if.uff.br

[1] A. Utzolino and K. Bluhm, Z. Naturforsch. B **51**, 912 (1996).
[2] J.C. Fernandes, F.S. Sarrat, R.B. Guimarães, R.S. Freitas, M.A. Continentino, A.C. Doriguetto, Y.P. Mascarenhas, J. Ellena, E.E. Castellano, J-L. Tholence, J. Dumas, and L. Ghivelder, Phys. Rev. B **67**, 104413 (2003).
[3] L.C. Tippie and W.G. Clark, Phys. Rev. B **23**, 5854 (1981).
[4] D.S. Fisher, Phys. Rev. B **50**, 3799 (1994); A. Saguia, B. Boechat, and M.A. Continentino, *ibid.* **62**, 5541 (2000); S. Bergkvist, P. Henelius, and A. Rosengren, *ibid.* **66**, 134407 (2002).
[5] H.M. Bozler, C.M. Gould, T.J. Bartolac, W.G. Clark, K. Glover, and J. Sanny, Bull. Am. Phys. Soc. **25**, 217 (1980).
[6] R.B. Guimarães, J.C. Fernandes, M.A. Continentino, H.A. Borges, C.S. Moura, J.B.M. da Cunha, and C.A. dos Santos, Phys. Rev. B **56**, 292 (1997).
[7] M.L. Siqueira, R.E. Rapp, and R. Calvo, Phys. Rev. B **48**, 3257 (1993).
[8] J.C. Ho and N.E. Phillips, Phys. Lett. **10**, 34 (1964).
[9] L.C. Tippie and W.G. Clark, Phys. Rev. B **23**, 5846 (1981).
[10] M.A. Continentino, J. Phys. C **16**, L71 (1983).
[11] A. Saguia, B. Boechat, and M.A. Continentino, Phys. Rev. Lett. **89**, 117202 (2002).